

# The influence of magnetic anisotropy on magnetoelectric behavior in conical spin ordered multiferroic state

Xiaoyan Yao,<sup>1,a)</sup> Veng Cheong Lo,<sup>2</sup> and Jun-Ming Liu<sup>3</sup>

<sup>1</sup>*Department of Physics, Southeast University, Nanjing 211189, China*

<sup>2</sup>*Department of Applied Physics, The Hong Kong Polytechnic University, Hong Kong, China*

<sup>3</sup>*Nanjing National Laboratory of Microstructures, Nanjing University, Nanjing 210093, China*

(Received 27 January 2010; accepted 24 March 2010; published online 6 May 2010)

For the magnetism-driven multiferroic materials, the magnetic anisotropy plays an essential role in the magnetoelectric behavior. To understand the influence of magnetic anisotropy on multiferroic state resulting from the conical spin order, we have performed Monte Carlo simulation on a three-dimensional classical Heisenberg model in spinel lattice. The single-ion anisotropy from the easy-axis type to the easy-plane type is considered in the system, and the corresponding magnetoelectric behavior is investigated under a rotating external magnetic field ( $\mathbf{h}$ ). It is revealed that the magnetic anisotropy drags the orientation of conical spin structure slightly away from the direction of  $\mathbf{h}$ , and distorts the conical spin structure as well. The balance between  $\mathbf{h}$  and the anisotropy results in the anisotropic magnetoelectric properties during the rotation of  $\mathbf{h}$ . © 2010 American Institute of Physics. [doi:10.1063/1.3407541]

## I. INTRODUCTION

Magnetoelectric (ME) materials in which magnetism and ferroelectricity coexist and mutually interact, have attracted considerable attention since the 1960s. This field becomes more appealing when the ferroelectric behavior appears to be connected with the magnetic order and can be manipulated by using an external magnetic field ( $\mathbf{h}$ ) in some frustrated compounds. Various magnetic controls of ferroelectric behavior have been observed, such as flop, reversal, rotation of ferroelectric polarization ( $\mathbf{P}$ ), and the anomaly of dielectric constant,<sup>1,2</sup> which inspire tremendous interest in both theoretical and experimental investigations due to the great potential for applications. In these frustrated materials, the ferroelectricity is always induced by some special magnetic orders with the collapse of inversion symmetry, such as the collinear up-up-down-down magnetic order<sup>3-5</sup> and noncollinear spiral spin state.<sup>6-8</sup> It is noted that the anisotropy is an important factor to affect the magnetic structure, and thus plays a key role on the magnetism-driven ferroelectric behavior. Therefore, the investigation on the anisotropy is very helpful to understand the ME behavior of magnetic origin.

Since it has been first confirmed in the experiment of  $\text{CoCr}_2\text{O}_4$  that the conical spin order can induce the fascinating multiferroicity with the coexistence of both spontaneous magnetization ( $\mathbf{M}$ ) and  $\mathbf{P}$ , the conical spin structure, as one type of noncollinear spin orders, attracts a lot of attention recently. In the conical spin order, the homogeneous components of spins along the conical axis produce  $\mathbf{M}$ , while their spiral parts give rise to  $\mathbf{P}$  according to the spin current model.<sup>9,10</sup> This inherent  $\mathbf{M}$ - $\mathbf{P}$  coupling provides a mechanism to realize various magnetic controls of ferroelectricity.<sup>11-16</sup> In particular, the continuous rotation of  $\mathbf{P}$  controlled by  $\mathbf{h}$  has been observed in some compounds in different structures, such as  $\text{Ba}_2\text{Mg}_2\text{Fe}_{12}\text{O}_{22}$ ,  $\text{ZnCr}_2\text{Se}_4$ , and

$\text{Eu}_{0.55}\text{Y}_{0.45}\text{MnO}_3$ .<sup>12,14,15</sup> It is noteworthy that in the experiments  $\mathbf{P}$  does not present a well-defined sinusoidal curve upon the rotating  $\mathbf{h}$  as expected in simulation.<sup>17</sup> The discrepancy is argued to be attributed to a weak magnetic anisotropy. The corresponding microscopic mechanism remains an interesting question.

In this paper, focusing on the influence of magnetic anisotropy on ME behavior in the conical spin state, we perform Monte Carlo simulation on a three-dimensional (3D) classical Heisenberg spin model in spinel structure. The single-ion anisotropy from the easy-axis type to the easy-plane type is considered. By applying a rotating  $\mathbf{h}$ , we explore the anisotropic ME response in detail. It is observed that the magnetic anisotropy not only drags the orientation of conical spin structure slightly away from the direction of  $\mathbf{h}$ , but also affects the shape of spin structure, which induces the different magnetic and ferroelectric behaviors under different anisotropies. The results obtained provide a wide-use principle for the anisotropic ME behavior in the conical spin ordered multiferroic state, which can be generally applied to the inherent or  $\mathbf{h}$ -induced conical spin structure observed in different materials with weak magnetic anisotropy.

## II. MODEL AND SIMULATION

Since the conical spin order observed in the spinel structure is inherent and stable even at  $\mathbf{h}=0$ , the present simulation is performed on a spinel lattice to produce the conical spin structure. The cubic spinel structure has the general formula  $\text{AB}_2\text{O}_4$  where  $B$  sites are arranged in pyrochlore sublattice while  $A$  sites form a diamond sublattice. These two sublattices interpenetrate into each other to construct the spinel structure. Previous investigations indicate that only the nearest-neighbor antiferromagnetic  $A$ - $B$  and  $B$ - $B$  exchange interactions ( $J_{AB}$  and  $J_{BB}$ ) are sufficient to produce a conical spin state, and the conical spin order has the lowest energy out of possible spin configurations when  $0.6667 < J_{BB}/J_{AB}$

<sup>a)</sup>Electronic mail: yaoxiaoyan@gmail.com.

$< 0.9735$ .<sup>18–21</sup> Therefore the values  $J_{BB} = -2.5$  and  $J_{AB} = -3$  are chosen in the present simulation. The single-ion anisotropy with the strength  $K$  along  $z$ -axis is taken into account.<sup>11</sup> By including the magnetic and electric energies, the total Hamiltonian can be written as

$$H = -J_{BB} \sum_{[i,j]} \mathbf{S}_{Bi} \cdot \mathbf{S}_{Bj} - J_{AB} \sum_{[i,j]} \mathbf{S}_{Ai} \cdot \mathbf{S}_{Bj} - K \sum_i [(S_{Bi}^z)^2 + (S_{Ai}^z)^2] - \mathbf{h} \cdot \mathbf{M} - \mathbf{E} \cdot \mathbf{P}, \quad (1)$$

where  $\mathbf{S}_{Ai}$  and  $\mathbf{S}_{Bi}$  are  $i$ th classical vector spins on  $A$  and  $B$  sites with unit magnitude.  $[i, j]$  denotes the summation over all the nearest-neighboring spin pairs for  $B$ – $B$  and  $A$ – $B$  sites in the spinel structure. Here  $\mathbf{E}$  is the external electric field and  $\mathbf{M}$  is evaluated as

$$\mathbf{M} = \sum_i (\mathbf{S}_{Ai} + \mathbf{S}_{Bi}). \quad (2)$$

According to the spin current model, or equivalently, in terms of the theory of inverse Dzyaloshinskii–Moriya interaction,<sup>9,10</sup>  $\mathbf{P}$  is induced by the neighboring canting spins ( $\mathbf{S}_i$  and  $\mathbf{S}_j$ ) as follows:

$$\mathbf{P} = -a \mathbf{e}_{ij} \times (\mathbf{S}_i \times \mathbf{S}_j), \quad (3)$$

where  $\mathbf{e}_{ij}$  denotes the vector connecting the two sites of  $\mathbf{S}_i$  and  $\mathbf{S}_j$ , namely in the direction of magnetic modulation vector  $\mathbf{k}$ . For convenience, only spin current between spins of  $B$  site is considered, and the factor  $a$  is assumed to be unity. Thus the total  $\mathbf{P}$  is written as

$$\mathbf{P} = - \sum_{[i,j]} \mathbf{e}_{ij} \times (\mathbf{S}_{Bi} \times \mathbf{S}_{Bj}). \quad (4)$$

The Monte Carlo simulation is performed on a 3D spinel lattice with the periodic boundary condition. The system size is  $L \times L \times L$  where  $L = 36$ . It is assumed that  $x$ ,  $y$ , and  $z$  axes are, respectively, along the direction of  $[100]$ ,  $[010]$ , and  $[001]$  in the spinel structure. The spin is updated according to the Metropolis algorithm and only the low temperature behaviors ( $T = 0.01$ ) are focused. Similar to the ME poling procedure prior to the measurement in the experiments,<sup>11,16</sup> the system is initially poled by an electric field  $\mathbf{E} = 0.707$  along  $[110]$  and a magnetic field  $\mathbf{h} = 1.5$  along  $[001]$  in simulation. This ME poling procedure produces a single ME domain with the conical spin structure appearing in the chains of  $B$  site, and the magnetic modulation vector  $\mathbf{k}$  is aligned along  $[1\bar{1}0]$ . After the ME poling process,  $\mathbf{E}$  is removed, and then starting from the polarized direction  $[001]$ ,  $\mathbf{h}$  is rotated by  $2\pi$  in the plane normal to  $\mathbf{k}$  with a fixed magnitude  $|\mathbf{h}| = 1.5$ .  $\mathbf{M}$  and  $\mathbf{P}$  are calculated at different  $\theta$  where  $\theta$  is the angle between  $z$ -axis and  $\mathbf{h}$ , as shown in Fig. 1(a). For every  $\mathbf{h}$  direction, the initial 10 000 Monte Carlo steps (MCSs) are discarded for equilibration, and then the results are obtained by averaging 1000 data. Each datum is collected at every ten MCSs. The final results are obtained by averaging independent data sets calculated by selecting different seeds for random number generation.

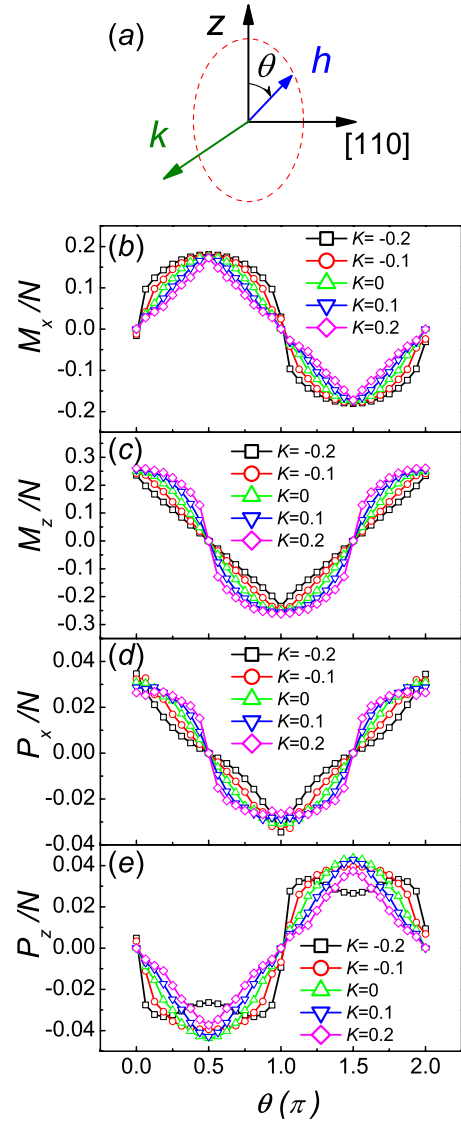


FIG. 1. (Color online) (a) The sketch shows that the magnetic field  $\mathbf{h}$  rotates within the plane normal to the magnetic modulation vector  $\mathbf{k}$ , where  $\theta$  is defined as the angle between the  $z$ -axis and the orientation of  $\mathbf{h}$ . (b)  $x$ -component of the magnetization  $\mathbf{M}$  ( $M_x$ ) and (c)  $z$ -component of  $\mathbf{M}$  ( $M_z$ ) as functions of  $\theta$  for the different magnitudes of single-ion anisotropy, namely  $K = -0.2, -0.1, 0, 0.1, \text{ and } 0.2$ . (d)  $x$ -component and (e)  $z$ -component of the ferroelectric polarization  $\mathbf{P}$ , namely  $P_x$  and  $P_z$ , as functions of  $\theta$  for  $K = -0.2, -0.1, 0, 0.1, \text{ and } 0.2$ . The  $\theta$  dependence of  $M_y$  ( $P_y$ ) is the same to that of  $M_x$  ( $P_x$ ) due to the crystal symmetry. Here  $N$  is the total number of magnetic ions.

### III. RESULTS AND DISCUSSION

Figures 1(b)–1(e) present  $\mathbf{M}$  and  $\mathbf{P}$  of the system with different  $K$  varying from  $-0.2$  to  $0.2$  during the rotation of  $\mathbf{h}$ . In the absence of anisotropy, i.e.,  $K = 0$ , all the three components of  $\mathbf{M}$  and  $\mathbf{P}$  demonstrate the curves in simple harmonic wave-form, implying that  $\mathbf{M}$  and  $\mathbf{P}$  rotate with  $\mathbf{h}$  simultaneously without any noticeable decay. The orientation of  $\mathbf{M}$  strictly follows  $\mathbf{h}$  at all times while that of  $\mathbf{P}$  is always perpendicular to  $\mathbf{h}$ . The presence of the single-ion anisotropy produces obvious effect on this ME behavior. Although the components of  $\mathbf{M}$  and  $\mathbf{P}$  still show the well-defined cyclic varying behavior, their shapes are no longer simple harmonic. With  $K$  changing from  $-0.2$  to  $0.2$ , the behavior of  $\mathbf{M}$

varies gradually and regularly. For the easy-axis anisotropy with  $K > 0$ , at  $\theta$  around 0 or  $\pi$ , namely  $\mathbf{h}$  along  $z$ -axis,  $M_z$  presents a broad crest, and simultaneously  $M_x(M_y)$  changes linearly crossing zero. At  $\theta = \pi/2$  or  $3\pi/2$  where  $\mathbf{h}$  is aligned parallel or antiparallel to  $[110]$ ,  $M_z$  varies sharply with its sign changed while  $M_x(M_y)$  presents a cusp. On the contrary, for the easy-plane anisotropy with  $K < 0$ ,  $M_x(M_y)$  shows a broad crest at  $\theta$  near  $\pi/2$  or  $3\pi/2$ , and changes the sign abruptly at  $\theta = 0$  and  $\pi$ . At the same time,  $M_z$  presents a cusplike extremum around  $\theta = 0$  or  $\pi$ , and varies linearly crossing zero at  $\theta = \pi/2$  and  $3\pi/2$ . As  $K$  varies,  $\mathbf{P}$  also presents the gradually changing curve with its orientation kept perpendicular to  $\mathbf{M}$ , namely,  $P_x(P_y)$  shows the similar behavior to that of  $M_z$  and the curve of  $P_z$  is similar to that of  $M_x(M_y)$ . The analogous ME response deviating from the sinusoidal-like curve has been observed in the experiments of  $\text{Eu}_{0.55}\text{Y}_{0.45}\text{MnO}_3$  and  $\text{Ba}_2\text{Mg}_2\text{Fe}_{12}\text{O}_{22}$ , etc.<sup>12,14</sup>

In order to explore this anisotropic ME properties upon rotating  $\mathbf{h}$ , the microscopic spin structure is investigated in detail. For convenience, we use the spin cone to characterize the conical spin structure. That is, if all the ionic sites in the chain along  $\mathbf{k}$  are moved to one site, then the spin vectors will lie on a surface of cone, namely a spin cone, as presented in Fig. 2(a). At  $\theta = 0$ , the homogeneous components along the cone axis produce a net  $\mathbf{M}$  along  $[001]$ , while the other components of spins rotate counterclockwise in the  $xy$ -plane along  $\mathbf{k}$ , giving rise to  $\mathbf{P}$  along  $[110]$ . The midpoint of cone bottom ( $C$ ) is scrutinized under different  $K$  to present the orientation of spin cone during  $\mathbf{h}$  rotation. Figures 2(b) and 2(c) display the coordinates of  $C$  as functions of  $\theta$ , which show almost the same curves to those of  $\mathbf{M}$ . The curve of  $C$  with  $K = 0$  in the shape of simple harmonic wave indicates that without anisotropy the axis of spin cone keeps to the direction of  $\mathbf{h}$  all along. When  $K \neq 0$ , the coordinates of  $C$  show the behaviors deviating from those of  $K = 0$ , which means that the axis of spin cone does not coincide with the orientation of  $\mathbf{h}$  under the effect of anisotropy. In order to show this deviation more clearly, the angle ( $\varphi$ ) from  $[001]$  to the conical axis is calculated for different  $\theta$ . As illustrated in Fig. 2(d), when  $K = 0$ ,  $\varphi$  is always equal to  $\theta$ . When  $K \neq 0$ ,  $\varphi$  is no longer equal to  $\theta$  except that  $\theta$  is integral multiples of  $\pi/2$ . In the  $\theta$  range from 0 to  $\pi/2$ ,  $\varphi$  is larger than  $\theta$  for  $K < 0$  but less than  $\theta$  when  $K > 0$ , which is just opposite to the case in the range from  $\pi/2$  to  $\pi$ . Besides, at  $K > 0$   $\varphi$  varies sharply at  $\theta = \pi/2$ , but changes gradually around  $\theta = 0$ . For  $K < 0$ , the trends are exactly opposite. This anisotropic behavior is caused by the competition between Zeeman energy and the anisotropy energy. The anisotropy of easy-axis type forces the spin to align along  $z$ -axis. Therefore, the axis of spin cone prefers to stay around  $\theta = 0$  or  $\pi$  but quickly flees away at  $\theta = \pi/2$  or  $3\pi/2$ , and thus it always lags behind  $\mathbf{h}$  below  $\pi/2$  but leads ahead of  $\mathbf{h}$  above  $\pi/2$ . In contrast, for the anisotropy of easy-plane type, namely the spin preferentially lies within  $xy$ -plane, the axis of spin cone tends to stay around  $\theta = \pi/2$  or  $3\pi/2$  but not along  $z$ -axis, and hence the result opposite to  $K > 0$  case is induced. Similar angular deviating behavior has also been observed in the experiment of Ref. 14. It is worthwhile to note that the components of  $\mathbf{M}$  show almost the same behaviors to the coordinates of  $C$ , indicating that the anisotropic behavior of  $\mathbf{M}$  just results from the deviation of the conical axis from the direction of  $\mathbf{h}$ .

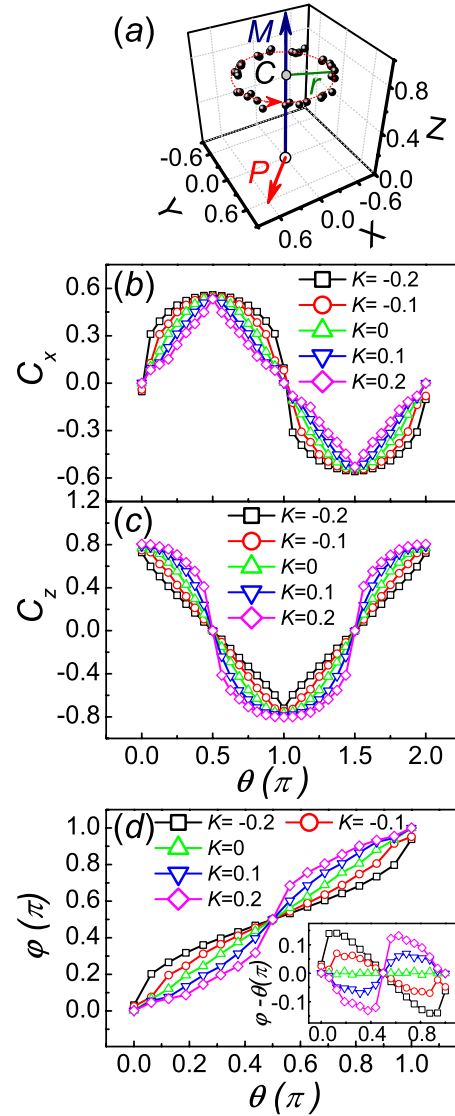


FIG. 2. (Color online) (a) The 3D snapshot for spin cone at  $K = 0$  and  $\theta = 0$  after ME poling procedure with the electric field  $\mathbf{E}$  removed. Here the dot represents the position of the top of spin vector with its bottom moved to zero. The arrow on the edge of cone shows that the spins in the chain rotate counterclockwise along  $\mathbf{k}$ . This conical spin state produces  $\mathbf{M}$  along  $[001]$  and  $\mathbf{P}$  along  $[110]$ . (b)  $x$ -coordinate and (c)  $z$ -coordinate of the midpoint of cone bottom ( $C$ ), namely  $C_x$  and  $C_z$ , as functions of  $\theta$  for  $K$  ranged from  $-0.2$  to  $0.2$ . The  $\theta$  dependence of  $C_y$  is the same to that of  $C_x$  due to the crystal symmetry. (d) The angle ( $\varphi$ ) from  $[001]$  to the conical axis is presented against  $\theta$  for different  $K$ . And the inset illustrates  $\varphi - \theta$ , namely the deviation of the conical axis from  $\mathbf{h}$  direction, as functions of  $\theta$  with different  $K$ .

coordinates of  $C$ , indicating that the anisotropic behavior of  $\mathbf{M}$  just results from the deviation of the conical axis from the direction of  $\mathbf{h}$ .

Besides the deviation of conical axis, the anisotropy also affects the shape of spin structure. To characterize the shape of spin cone, the average radius ( $r_{\text{ave}}$ ), maximal radius ( $r_{\text{max}}$ ) and minimal radius ( $r_{\text{min}}$ ) of spin cone are monitored during the whole rotation of  $\mathbf{h}$  for different  $K$ . As illustrated in Fig. 3(c), at  $K = 0$ ,  $r_{\text{ave}}$ ,  $r_{\text{max}}$ , and  $r_{\text{min}}$  coincides with each other and keep almost invariant in the whole course of rotating  $\mathbf{h}$ , which means that the spin cone is well reserved as a whole without anisotropy. Introducing the different anisotropy in-

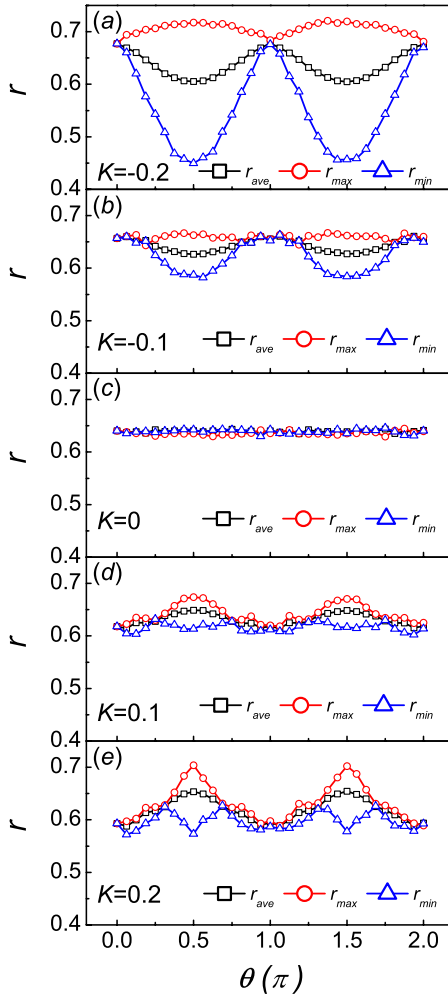


FIG. 3. (Color online) The average radius ( $r_{\text{ave}}$ ), maximal radius ( $r_{\text{max}}$ ), and minimal radius ( $r_{\text{min}}$ ) of spin cone as functions of  $\theta$  for (a)  $K=-0.2$ , (b)  $K=-0.1$ , (c)  $K=0$ , (d)  $K=0.1$ , and (e)  $K=0.2$ .

duces the different variations in  $r_{\text{ave}}$ ,  $r_{\text{max}}$  and  $r_{\text{min}}$  upon the rotating  $\mathbf{h}$ , which means that the spin-structural transformation occurs in different ways for different  $K$ . At  $\theta=0$ ,  $r_{\text{ave}}=r_{\text{max}}=r_{\text{min}}$ , namely, the spin structure is always in the shape of a regular cone for different  $K$ . The conical shape is slimmer for  $K>0$  but flatter for  $K<0$ . Thus the spin components in the spiral plane are larger when  $K$  is smaller, leading to the higher  $\mathbf{P}$  presented in Fig. 1(d). As  $\mathbf{h}$  is rotated, the emerging difference between  $r_{\text{max}}$  and  $r_{\text{min}}$  reflects that the spin cone is distorted by the magnetic anisotropy when  $\mathbf{h}$  deviates from  $z$ -axis, and this effect is enhanced by a stronger anisotropy. The distortion of spin cone reaches the maximum at  $\theta=\pi/2$  and  $3\pi/2$ . It is illustrated in the snapshot of spin configuration (Fig. 4) that the distorted elliptical spin cone is actually formed. The easy-axis anisotropy stretches the spin cone toward  $z$ -axis while the easy-plane anisotropy suppresses the spin cone toward  $xy$ -plane. The distortion of spin cone affects the detailed behavior of  $\mathbf{P}$ , i.e.,  $\mathbf{P}$  is suppressed at  $\theta=\pi/2$  and  $3\pi/2$  in both cases with  $K<0$  and  $K>0$ , which is different to the behavior of  $\mathbf{M}$ .

It should be mentioned that if the anisotropy is too strong the conical spin structure will be ultimately destroyed. Therefore, only weak anisotropy is considered here to inves-

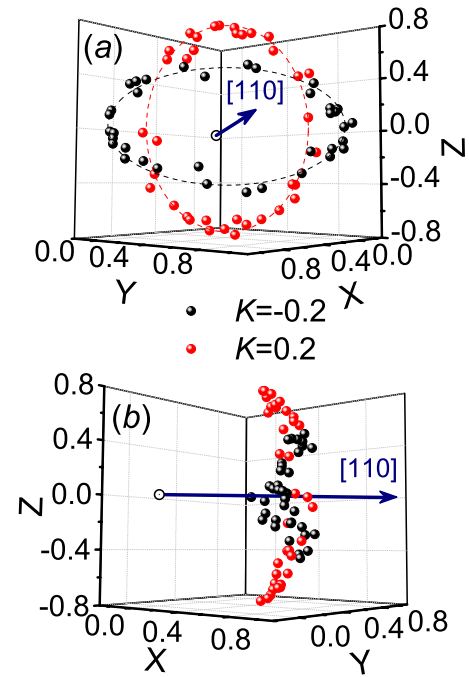


FIG. 4. (Color online) (a) and (b) The snapshots of spin cone at  $\theta=\pi/2$  for  $K=-0.2$  and  $0.2$  represented by dots with different colors, which are viewed in different directions.

tigate the ME behavior in conical spin ordered state. It is revealed that  $\mathbf{P}$  can be rotated by  $\mathbf{h}$  upon weak  $K$ , which is attributed to the conical spin structure almost reserved during  $\mathbf{h}$  rotation. However, even under weak anisotropy, the shape and movement of spin cone will be influenced, and thus the magnetic and ferroelectric properties are very sensitive to the anisotropy. The deviation of the cone axis from the direction of  $\mathbf{h}$  leads to the anisotropic behavior of  $\mathbf{M}$ , while the anisotropic behavior of  $\mathbf{P}$  results from both the deviation and distortion of spin cone. It has been observed that the magnetic anisotropy is weak in some compounds with the spinel structure or spinel layers,<sup>12,20</sup> which ensures that the continuous  $\mathbf{h}$ -control of ferroelectricity may be realized, and the corresponding anisotropic ME behavior can be well understood by the present work.

#### IV. CONCLUSION

In summary, aiming at ME phenomenon under the influence of the magnetic anisotropy in the conical spin ordered multiferroics, we have investigated the variation in magnetic and ferroelectric behaviors under rotating  $\mathbf{h}$ . The Monte Carlo simulation is performed based on a classical Heisenberg model in spinel structure with the single-ion anisotropy from the easy-axis type to the easy-plane type. Different ME responses to  $\mathbf{h}$  are observed under different  $K$ . The detailed analysis on spin configuration reveals that the anisotropic energy competing with Zeeman energy not only determines the orientation of spin cone but also influences its shape. The deviation of cone axis from  $\mathbf{h}$  leads to the  $\theta$ -dependences of  $\mathbf{M}$  and  $\mathbf{P}$  deviating from the sinusoidal curve, and the distortion of spin cone causes the additive detailed change of  $\mathbf{P}$ . The results obtained provide more insights into the conical magnetic ordered multiferroic state with different anisotropy,

which can be generally applied to not only the inherent conical spin order in spinel structure but also  $h$ -induced conical spin state observed in other materials.

## ACKNOWLEDGMENTS

This work is supported by the research grants from the National Natural Science Foundation of China (Grant No. 10904014), and supported by the computational center from Department of Physics, Southeast University.

<sup>1</sup>K. F. Wang, J.-M. Liu, and Z. F. Ren, *Adv. Phys.* **58**, 321 (2009).

<sup>2</sup>S.-W. Cheong and M. Mostovoy, *Nat. Mater.* **6**, 13 (2007).

<sup>3</sup>Y. J. Choi, H. T. Yi, S. Lee, Q. Huang, V. Kiryukhin, and S.-W. Cheong, *Phys. Rev. Lett.* **100**, 047601 (2008).

<sup>4</sup>X. Yao and V. C. Lo, *J. Appl. Phys.* **104**, 083919 (2008).

<sup>5</sup>X. Yao, V. C. Lo, and J.-M. Liu, *J. Appl. Phys.* **105**, 033907 (2009).

<sup>6</sup>T. Kimura, T. Goto, H. Shintani, K. Ishizaka, T. Arima, and Y. Tokura, *Nature (London)* **426**, 55 (2003).

<sup>7</sup>K. Taniguchi, N. Abe, T. Takenobu, Y. Iwasa, and T. Arima, *Phys. Rev. Lett.* **97**, 097203 (2006).

<sup>8</sup>S. Park, Y. J. Choi, C. L. Zhang, and S.-W. Cheong, *Phys. Rev. Lett.* **98**, 057601 (2007).

<sup>9</sup>H. Katsura, N. Nagaosa, and A. V. Balatsky, *Phys. Rev. Lett.* **95**, 057205 (2005).

<sup>10</sup>I. A. Sergienko and E. Dagotto, *Phys. Rev. B* **73**, 094434 (2006).

<sup>11</sup>Y. J. Choi, J. Okamoto, D. J. Huang, K. S. Chao, H. J. Lin, C. T. Chen, M. van Veenendaal, T. A. Kaplan, and S.-W. Cheong, *Phys. Rev. Lett.* **102**, 067601 (2009).

<sup>12</sup>S. Ishiwata, Y. Taguchi, H. Murakawa, Y. Onose, and Y. Tokura, *Science* **319**, 1643 (2008).

<sup>13</sup>I. Kim, Y. S. Oh, Y. Liu, S. H. Chun, J.-S. Lee, K.-T. Ko, J.-H. Park, J.-H. Chung, and K. H. Kim, *Appl. Phys. Lett.* **94**, 042505 (2009).

<sup>14</sup>H. Murakawa, Y. Onose, F. Kagawa, S. Ishiwata, Y. Kaneko, and Y. Tokura, *Phys. Rev. Lett.* **101**, 197207 (2008).

<sup>15</sup>H. Murakawa, Y. Onose, K. Ohgushi, S. Ishiwata, and Y. Tokura, *J. Phys. Soc. Jpn.* **77**, 043709 (2008).

<sup>16</sup>Y. Yamasaki, S. Miyasaka, Y. Kaneko, J.-P. He, T. Arima, and Y. Tokura, *Phys. Rev. Lett.* **96**, 207204 (2006).

<sup>17</sup>X. Yao and Q. Li, *EPL* **88**, 47002 (2009).

<sup>18</sup>G. Lawes, B. Melot, K. Page, C. Ederer, M. A. Hayward, T. Proffen, and R. Seshadri, *Phys. Rev. B* **74**, 024413 (2006).

<sup>19</sup>C. Ederer and M. Komelj, *Phys. Rev. B* **76**, 064409 (2007).

<sup>20</sup>T. A. Kaplan, K. Dwight, D. Lyons, and N. Menyuk, *J. Appl. Phys.* **32**, S13 (1961).

<sup>21</sup>D. H. Lyons, T. A. Kaplan, K. Dwight, and N. Menyuk, *Phys. Rev.* **126**, 540 (1962).